

Appendix 1

Methods

Random noise was iteratively introduced within k-space of an open-source agar-based phantom dataset. The process involved transforming the complex MRE data into k-space data through Fourier Transform (FT). Subsequently, random noise was introduced, with levels ranging from 0 to 2 times the standard deviation of the original image using 40 iterations. Finally, another FT was applied to the noisy k-space to reconstruct the complex MRE data. The kMDEV inversion algorithm was employed, resulting in the generation of SWS maps. To determine mean SWS, displacement, OSS, and Laplacian-SNR, the same region-of-interest (ROI) was utilized for both the simulated motion experiments of the inclusions and background.

Results

Magnitude images and corresponding SWS maps with added random noise can be seen in Figure S1. The median SWS for each iteration of added random noise as a function of displacement-, OSS- and Laplacian-SNR are shown in Figure S2.

For the healthy volunteers a different number of motion states were used to investigate the effect of binning for each motion correction method. In Figure S3 an example of a healthy volunteer is shown with nine motion states shown consecutively after binning of each imaging slice based on the height in the breathing signal. The average ROI size in healthy volunteers was 574 ± 302 voxels for the pancreas and $3,042 \pm 1,428$ voxels in the kidney.

Discussion

Simulated noise was incorporated within a MRE dataset of a static phantom with known stiffness inclusions. The addition of noise in k-space resulted in a rapid decrease of measured SWS around 0.5 m/s, indicating that SNR has a significant effect on the measured SWS. Similarly, McGarry et al. showed deviations from the ground truth with the measured shear modulus in a gelatin phantom for OSS-SNR values below 4 dB for soft inclusions (~3.3 kPa) and 10 dB for stiff inclusions (~8.8 kPa) (20). Triolo *et al.* observed the same effect of the apparent absolute shear modulus increasing for higher OSS-SNR after denoising (30).

References

30. Triolo ER, Khagai O, Veraart J, Alipour A, Balchandani P, Kurt M. How signal-to-noise ratio impacts the apparent stiffness of brain tissue in MR Elastography at 7T. Summer Biomechanics, Bioengineering and Biotransport Conference June 20-23, Eastern Shore, MD, USA, 2022.

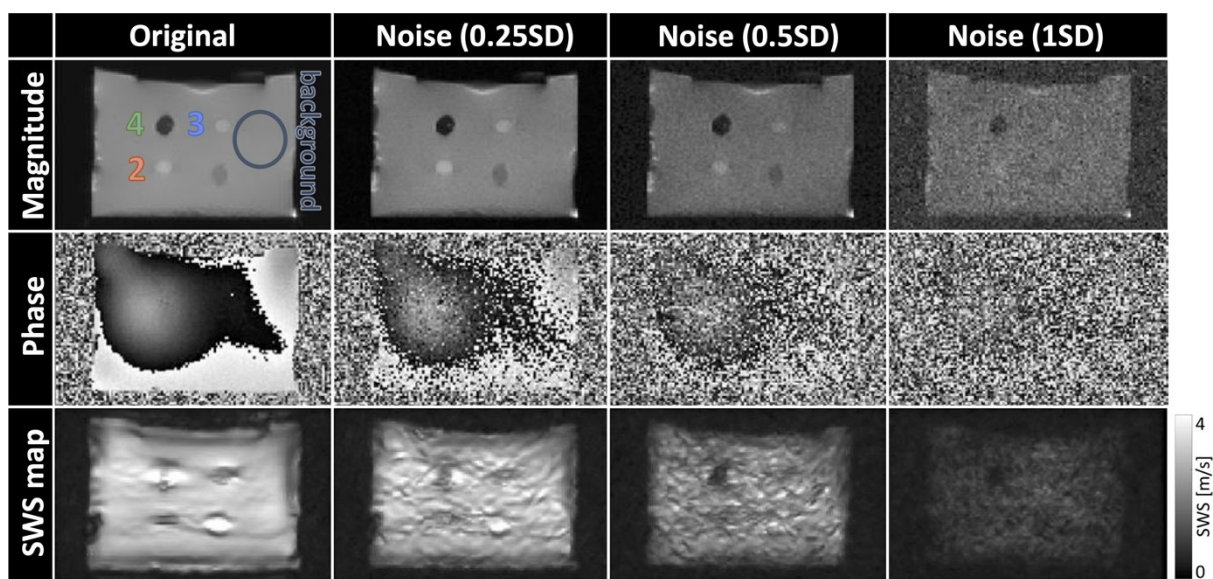


Figure S1 The magnitude image of the phantom with the inclusions highlighted by number and background highlighted by the circle (top) for the static MRE phantom dataset (original), after addition of random noise in k-space with 0.25 times the SD, after adding random noise at 0.5 SD, and after random noise at 1.0 SD. The corresponding phase images (middle) and SWS maps (bottom) are shown. SWS, shear wave speed; SD, standard deviation; MRE, magnetic resonance elastography.

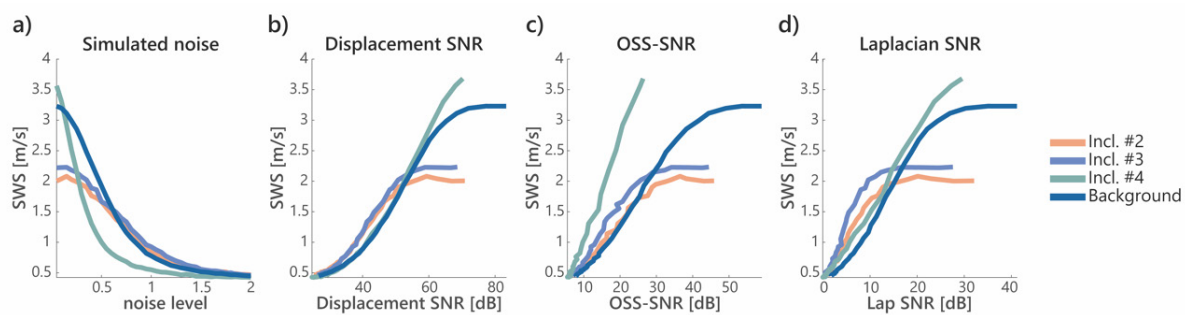


Figure S2 Mean SWS per inclusion and background as a function of (A) the level of added noise. The SNR values are calculated per noise level and plotted as a function of (B) displacement SNR, (C) OSS SNR, (D) Laplacian SNR. SNR, signal-to-noise ratio; OSS, octahedral shear strain; SWS, shear wave speed.

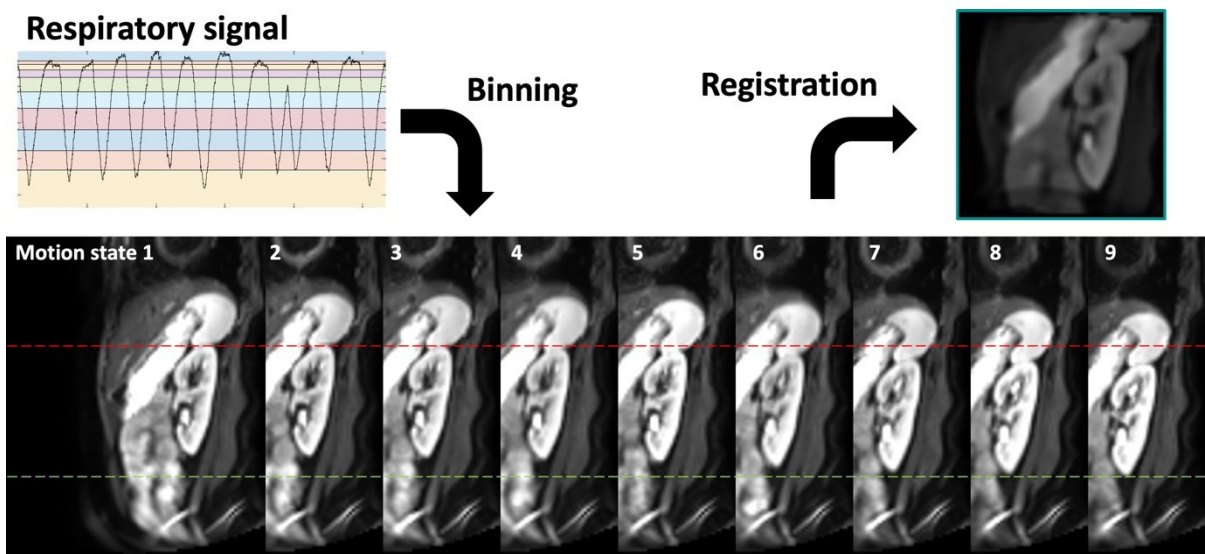


Figure S3 An example of a healthy volunteer with (top) the respiratory signal binned in nine motion states (bottom) upon which motion correction can be used to register each motion state to end expiration and create motion resolved complex MRE data. MRE, magnetic resonance elastography.